Supporting Information for: A strong non-equilibrium bound for sorting of crosslinkers on growing biopolymers

Yuqing Qiu, Michael Nguyen, Glen M. Hocky, Aaron R. Dinner, Suriyanarayanan Vaikuntanathan

S1. MEAN-FIELD MASTER EQUATION

A. The backward rates in the master equation account for conditional probabilities during unbinding

We summarize the rates used in the master equation in Table S1. While in the KMC simulations the backward rates are unity, in the master equation they include the conditional probabilities of finding the appropriate type of ABP during unbinding. We thus express them in terms of the domain lengths in the bulk. To validate these expressions, we compute the effective backward rates in KMC simulations by counting the number of occurrences of each unbinding case. Fig. S1 demonstrates that the expressions are quantitatively accurate.

Table S1. Forward and Backward rates for ABP in Master Equation (ME) and KMC Simulations

	Forward Rates	ME and KMC	Backward Rates	ME	KMC
First head of ABP	$k^{f,1}_{\alpha\alpha}$	$k^{f,1}_{\alpha\alpha} = k^{f,1}_{\beta\alpha}$	$k^{b',1}_{\alpha\alpha}$ or $k^{b,1}_{\alpha\alpha}$	1	1
	$k^{f,1}_{\alpha\beta}$		$k^{b',1}_{\alpha\beta}$ or $k^{b,1}_{\alpha\beta}$	1	1
	$k^{f,1}_{\beta\beta}$	$k^{f,1}_{\beta\beta} = k^{f,1}_{\alpha\beta}$	$k^{b',1}_{\beta\beta}$ or $k^{b,1}_{\beta\beta}$	1	1
	$k^{f,1}_{\beta\alpha}$		$k^{b',1}_{\beta\alpha}$ or $k^{b,1}_{\beta\alpha}$	1	1
Second head of ABP	$k^{f,2}_{\alpha\alpha}$		$k^{b',2}_{\alpha\alpha}$ or $k^{b,2}_{\alpha\alpha}$	$(L_\alpha - 1)/L_\alpha$	1
	$k^{f,2}_{\beta\alpha}$		$k^{b',2}_{\beta\alpha}$ or $k^{b,2}_{\beta\alpha}$	$1/L_\alpha$	1
	$k^{f,2}_{\beta\beta}$		$k^{b',2}_{\beta\beta}$ or $k^{b,2}_{\beta\beta}$	$(L_\beta - 1)/L_\beta$	1
	$k^{f,2}_{\alpha\beta}$		$k^{b',2}_{\alpha\beta}$ or $k^{b,2}_{\alpha\beta}$	$1/L_\beta$	1

B. Domain lengths and rates at equilibrium

Given the rates in Table S1, we can solve the master equation (Eq. (5)) at equilibrium to obtain constraints on the equilibrium rates. At equilibrium, all currents are zero, which results in the following relations between the equilibrium rates and equilibrium domain lengths, $L_{\alpha,\mathrm{eq}}$ and $L_{\beta,\mathrm{eq}}$.

$$\begin{aligned} k^{f,1}_{\alpha\alpha,eq} k^{f,2}_{\alpha\alpha,eq} &= \frac{L_{\alpha,eq} - 1}{L_{\alpha,eq}} \\ k^{f,1}_{\beta\beta,eq} k^{f,2}_{\beta\beta,eq} &= \frac{L_{\beta,eq} - 1}{L_{\beta,eq}} \\ k^{f,1}_{\alpha\beta,eq} k^{f,2}_{\alpha\beta,eq} k^{f,1}_{\beta\alpha,eq} k^{f,2}_{\beta\alpha,eq} &= \frac{1}{L_{\alpha,eq} L_{\beta,eq}} \end{aligned} \tag{S1}$$

Since $k^{f,1}_{\alpha\alpha,eq} = k^{f,1}_{\beta\alpha,eq}$ and $k^{f,1}_{\beta\beta,eq} = k^{f,1}_{\alpha\beta,eq}$, there are six independent forward rates at equilibrium. We use the

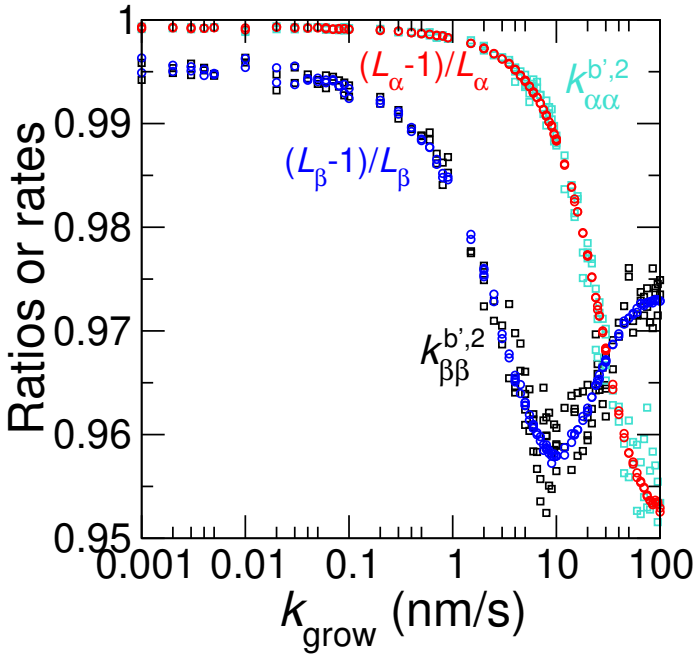

Figure S1. Validation of the backward rate expressions used in the master equation. The ratios of domain lengths $(L_\alpha - 1)/L_\alpha$ and $(L_\beta - 1)/L_\beta$ (blue and red circles) are computed from full bundle configurations in KMC simulations. The effective backward rates $k^{b',2}_{\alpha\alpha}$ (cyan) and $k^{b',2}_{\beta\beta}$ (black) in KMC simulations are computed as $k^{b',2}_{\alpha\alpha} = N^{b,2}_{\alpha\alpha}/(N^{b,2}_{\alpha\alpha} + N^{b,2}_{\beta\alpha})$ and $k^{b',2}_{\beta\beta} = N^{b,2}_{\beta\beta}/(N^{b,2}_{\alpha\beta} + N^{b,2}_{\beta\beta})$. $N^{b,2}_{ij}$ is the number of occurrences of unbinding the second head of an ABP, where i and j are the types of the last two ABPs at the tip.

constraints above but split the third equation in Eq. (S1) into the relations:

$$\begin{aligned} k^{f,1}_{\alpha\beta,eq} k^{f,2}_{\alpha\beta,eq} &= \frac{L_{\beta,\mathrm{eq}} - 1}{L_{\beta,\mathrm{eq}}(L_{\alpha,\mathrm{eq}} - 1)} \\ k^{f,1}_{\beta\alpha,eq} k^{f,2}_{\beta\alpha,eq} &= \frac{L_{\alpha,\mathrm{eq}} - 1}{L_{\alpha,\mathrm{eq}}(L_{\beta,\mathrm{eq}} - 1)}. \end{aligned} \tag{S2}$$

An interpretation of Eq. (S2) is that the effective mechanical penalty in switching from α to β is $k^{f,2}_{\alpha\beta,eq}/k^{f,2}_{\beta\beta,eq} = 1/(L_{\alpha,eq} - 1)$, and the bending penalty in switching from β to α is $k^{f,2}_{\beta\alpha,eq}/k^{f,2}_{\alpha\alpha,eq} = 1/(L_{\beta,eq} - 1)$. This is obtained by dividing equalities in Eq. (S2) by those in Eq. (S1).

We use these constraints on the equilibrium rates to simplify the expression for the entropy production (see SI Section 4). Using Eq. (S1) and Eq. (S2), we are able to represent the equilibrium condition with four parameters, $L_{\alpha,\mathrm{eq}}$, $L_{\beta,\mathrm{eq}}$, $k^{f,1}_{\alpha\alpha,\mathrm{eq}}$, and $k^{f,1}_{\beta\beta,eq}$.

C. Derivation of the self-consistency conditions

Under non-equilibrium conditions, the currents are non-zero. We need an additional constraint on the domain lengths to solve the master equation for L_α and L_β. For this purpose, we derive the following self-consistency conditions, which are inspired by Ref. [1]. Our derivation closely follows that of Ref. [1] and adapts it to this specific problem. The aim of this section is to provide a detailed overview for readers who are not familiar with this earlier work. We consider a chain of ABPs with the sequence of $\omega_l\omega_{l-1}...\omega_0$, where ω_i represents the type of ABP at position i. The notations introduced below use the following convention. The crosslinker at the tip is the last one in the sequence, *e.g.* index $i = 0$ is at the tip for the sequence of $\omega_l\omega_{l-1}...\omega_0$, and index $i = Z$ is at the tip for the sequence

of $\omega_{l-1}...\omega_0\omega_Z$. We write down an equation for the probability of finding this sequence at time t, $P^t(\omega_l\omega_{l-1}...\omega_0)$:

$$\begin{aligned}\frac{\partial P^t(\omega_l\omega_{l-1}...\omega_0)}{\partial t} &= w^+_{\omega_0|\omega_1}P^t(\omega_l\omega_{l-1}...\omega_1)\\ &+\sum_{\omega_Z} w^-_{\omega_Z|\omega_0}P^t(\omega_l\omega_{l-1}\omega_{l-2}...\omega_0\omega_Z)\\ &-(w^-_{\omega_0|\omega_1}+\sum_{\omega_Z} w^+_{\omega_Z|\omega_0})P^t(\omega_l\omega_{l-1}\omega_{l-2}...\omega_0),\end{aligned} \tag{S3}$$

$w^+_{\omega_i|\omega_j}$ is the rate of addition of ω_i to ω_j and $w^-_{\omega_i|\omega_j}$ is the rate of removal of ω_i to expose ω_j at the tip. In what follows, we solve Eq. (S3) at steady state:

$$\frac{\partial P^t(\omega_l\omega_{l-1}\omega_{l-2}...\omega_0)}{\partial t} = 0. \tag{S4}$$

The right hand side of Eq. (S3) contains probabilities of sequences with lengths l, $l+1$ and $l+2$. We simplify Eq. (S3) by rewriting the last two terms in terms of the probabilities of finding sequences with a fixed length l.

$$\begin{aligned}\frac{\partial P^t(\omega_l\omega_{l-1}...\omega_0)}{\partial t} &= w^+_{\omega_0|\omega_1}P^t(\omega_l\omega_{l-1}...\omega_1)\\ &+\sum_{\omega_Z} w^-_{\omega_Z|\omega_0}P^t(\omega_l|\omega_{l-1}\omega_{l-2}...\omega_0)P^t(\omega_{l-1}\omega_{l-2}...\omega_0|\omega_{l-2}\omega_{l-1}...\omega_0\omega_Z)P^t(\omega_{l-2}\omega_{l-1}...\omega_0\omega_Z)\\ &-(w^-_{\omega_0|\omega_1}+\sum_{\omega_Z} w^+_{\omega_Z|\omega_0})P^t(\omega_l|\omega_{l-1}\omega_{l-2}...\omega_0)P^t(\omega_{l-1}\omega_{l-2}...\omega_0),\end{aligned} \tag{S5}$$

where $P(\Gamma_x|\Gamma_y)$ is the conditional probability of generating sequence Γ_x given the sequence Γ_y. The sequence we consider is always in the following order $\omega_l\omega_{l-1}\omega_{l-2}...\omega_0\omega_Z$ where ω_l is in the bulk and ω_Z is at the tip. We then substitute Eq. (S5) into Eq. (S4) and rearrange to express the possibility of finding ω_l in addition to the sequence $\omega_{l-1}\omega_{l-2}...\omega_0$.

$$\begin{aligned}P^t(\omega_l|\omega_{l-1}\omega_{l-2}...\omega_0) &= \frac{w^+_{\omega_0|\omega_1}P^t(\omega_l\omega_{l-1}...\omega_1)}{(w^-_{\omega_0|\omega_1}+v_{\omega_0})P^t(\omega_{l-1}\omega_{l-2}...\omega_0)}\\ v_{\omega_0} &\equiv \frac{\sum_{\omega_Z} w^+_{\omega_Z|\omega_0}P^t(\omega_{l-1}\omega_{l-2}...\omega_0)-\sum_{\omega_Z} w^-_{\omega_Z|\omega_0}P^t(\omega_{l-1}\omega_{l-2}...\omega_0\omega_Z)}{P^t(\omega_{l-1}\omega_{l-2}...\omega_0)}\end{aligned} \tag{S6}$$

Physically, v_{ω_0} is the net growth rate at the tip with crosslinker type ω_0. By further rearranging Eq. (S6) and summing over ω_0, we obtain the following expression.

$$\sum_{\omega_0} w^+_{\omega_0|\omega_1}P^t(\omega_l\omega_{l-1}...\omega_1)-\sum_{\omega_0} w^-_{\omega_0|\omega_1}P^t(\omega_l\omega_{l-1}...\omega_0)=\sum_{\omega_0} v_{\omega_0}P^t(\omega_l|\omega_{l-1}\omega_{l-2}...\omega_0)P^t(\omega_{l-1}\omega_{l-2}...\omega_0) \tag{S7}$$

The left side of Eq. (S7) is $v_{\omega_1}P^t(\omega_l\omega_{l-1}...\omega_1)$, so Eq. (S7) becomes

$$v_{\omega_1}P^t(\omega_l\omega_{l-1}...\omega_1)=\sum_{\omega_0} v_{\omega_0}P^t(\omega_{l-1}\omega_{l-2}...\omega_0)P^t(\omega_l|\omega_{l-1}\omega_{l-2}...\omega_0). \tag{S8}$$

Eq. (S8) is equivalent to Eq. 34 in ref. [1] and connects the probabilities of observing various sequences at the tip.

We now proceed to connect the probabilities associated with observing configurations at the tip to the probabilities associated with observing configurations in the bulk (or far from the tip). The latter is relevant to us as these are the eventual correlations that can be observed after the polymer growth.

To proceed, we begin by writing down the following relation,

$$P^t_1(\Gamma_1)=\sum_{\Gamma_0} W(\Gamma_1,\Gamma_0)P^t_0(\Gamma_0) \tag{S9}$$

where we use Γ_0 to represent the configuration $\omega_{l-1}\omega_{l-2}...\omega_0$ and Γ_1 to represent the configuration $\omega_l\omega_{l-2}...\omega_1$. $P^t_1(\Gamma)$

represents the probability of observing a configuration Γ one unit away from the tip, $P_0^t(\Gamma)$ represents the probability of observing a configuration Γ starting at the tip, and $W(\Gamma_1, \Gamma_0) \equiv P^t(\omega_l|\omega_{l-1}\omega_{l-2}...\omega_0)$ is a transition matrix.

The matrix expression in Eq. S9, makes it easier to infer the eventual probability of observing patterns deep in the bulk of the assembly, away from the tip. Specifically, from Eq. S9, we can obtain an expression for the probability of observing a particular l length configuration N units away from the tip as

$$\mathbf{P}_N^t = W^N \mathbf{P}_0^t. \tag{S10}$$

where $\mathbf{P}_i^t$, denotes the probability vector associated with entries $P_i^t(\Gamma)$. In the limit $N \to \infty$, $\mathbf{P}_N^t$ will describe the probability of observing l length configurations deep in the bulk of the assembly. $\mathbf{P}_\infty^t$ can be connected to the properties of the transition matrix W by noting that the eigenvalues of W are ≤ 1 with an unique eigenvector with maximal eigenvalue 1. Hence, in the limit $N \to \infty$, the product $W^N \mathbf{P}_0^t$ is simply equal to maximal eigenvector $\bar{P}(\Gamma)$, components along all other eigenvectors decay away to zero. This eigenvector is the probability $\bar{P}(\Gamma)$ of finding a particular sequence Γ in the bulk.

From Eq S8, it is clear by substitution that $\bar{P}(\Gamma)$ satisfies

$$v_{\text{tip}}(\Gamma)P^t(\Gamma) = \bar{v}\bar{P}(\Gamma) \tag{S11}$$

$\bar{v}$ is the total growth rate at the tip for all configurations, and $v_{\text{tip}}(\Gamma_i \equiv \omega_{l-i-1}\omega_{l-i-2}...\omega_i) = v_{\omega_i}$. In what follows, we use Eq. (S11) to derive the self-consistency conditions specific to our system. We choose two neighboring ABPs $\omega_m\omega_{m-1}$ for the configuration size, where m ranges from 1 to l. There are four configurations: $\omega_{m,\alpha}, \omega_{m-1,\alpha}$, $\omega_{m,\beta}, \omega_{m-1,\alpha}$, $\omega_{m,\alpha}, \omega_{m-1,\beta}$, and $\omega_{m,\beta}, \omega_{m-1,\beta}$. We refer to the term on the right hand side of Eq. (S11) as currents in the main text.

$$\begin{aligned}
v_{\text{tip}}(\omega_{m,\alpha}, \omega_{m-1,\alpha})P^t(\omega_{m,\alpha}, \omega_{m-1,\alpha}) \equiv& J_{\omega_{m,\alpha},\omega_{m-1,\alpha}} \\
=& k_{\alpha\alpha}^{f,1}P(\alpha) - k_{\alpha\alpha}^{b,1}P(\alpha\alpha*) = k_{\alpha\alpha}^{f,2}P(\alpha\alpha*) - k_{\alpha\alpha}^{b,2}P(\alpha) \\
v_{\text{tip}}(\omega_{m,\beta}, \omega_{m-1,\beta})P^t(\omega_{m,\beta}, \omega_{m-1,\beta}) \equiv& J_{\omega_{m,\beta},\omega_{m-1,\beta}} \\
=& k_{\beta\beta}^{f,1}P(\beta) - k_{\beta\beta}^{b,1}P(\beta\beta*) = k_{\beta\beta}^{f,2}P(\beta\beta*) - k_{\beta\beta}^{b,2}P(\beta) \\
v_{\text{tip}}(\omega_{m,\alpha}, \omega_{m-1,\beta})P^t(\omega_{m,\alpha}, \omega_{m-1,\beta}) \equiv& J_{\omega_{m,\alpha},\omega_{m-1,\beta}} \\
=& k_{\alpha\beta}^{f,1}P(\alpha) - k_{\alpha\beta}^{b,1}P(\alpha\beta*) = k_{\alpha\beta}^{f,2}P(\alpha\beta*) - k_{\alpha\beta}^{b,2}P(\beta) \\
v_{\text{tip}}(\omega_{m,\beta}, \omega_{m-1,\alpha})P^t(\omega_{m,\beta}, \omega_{m-1,\alpha}) \equiv& J_{\omega_{m,\beta},\omega_{m-1,\alpha}} \\
=& k_{\beta\alpha}^{f,1}P(\beta) - k_{\beta\alpha}^{b,1}P(\beta\alpha*) = k_{\beta\alpha}^{f,2}P(\beta\alpha*) - k_{\beta\alpha}^{b,2}P(\alpha)
\end{aligned} \tag{S12}$$

where $J_{\omega_{m,i},\omega_{m-1,j}}$ is the current of ABPs of type j binding after ABPs of type i. J_{tot} is the sum of the four currents:

$$\bar{v} \equiv J_{\text{tot}} = J_{\omega_{m-1,\alpha},\omega_{m,\alpha}} + J_{\omega_{m-1,\alpha},\omega_{m,\beta}} + J_{\omega_{m-1,\beta},\omega_{m,\beta}} + J_{\omega_{m-1,\beta},\omega_{m,\alpha}}. \tag{S13}$$

By combining Eqs. (S11) to (S13), we can obtain the following self-consistency conditions,

$$\begin{aligned}
J_{\omega_{m-1,\alpha},\omega_{m,\alpha}} &= \bar{P}^t(\omega_{m,\alpha}, \omega_{m-1,\alpha})J_{\text{tot}} \\
J_{\omega_{m-1,\beta},\omega_{m,\beta}} &= \bar{P}^t(\omega_{m,\beta}, \omega_{m-1,\beta})J_{\text{tot}} \\
J_{\omega_{m-1,\alpha},\omega_{m,\beta}} = J_{\omega_{m-1,\beta},\omega_{m,\alpha}} &= \bar{P}^t(\omega_{m,\alpha}, \omega_{m-1,\beta})J_{\text{tot}}.
\end{aligned} \tag{S14}$$

The current $J_{\omega_{m-1,\alpha},\omega_{m,\beta}}$ is identical to the current $J_{\omega_{m-1,\beta},\omega_{m,\alpha}}$ because for every switch of a domain of α crosslinkers there is a switch to a domain of β crosslinkers. $\bar{P}^t(\omega_m, \omega_{m-1})$ is the probability of finding a specific configuration $\omega_m\omega_{m-1}$ in the bulk; it can be expressed in terms of the domain lengths as follows.

$$\begin{aligned}
\bar{P}^t(\omega_{m,\alpha}, \omega_{m-1,\alpha}) &= \frac{L_\alpha - 1}{L_\alpha + L_\beta} \\
\bar{P}^t(\omega_{m,\beta}, \omega_{m-1,\beta}) &= \frac{L_\beta - 1}{L_\alpha + L_\beta} \\
\bar{P}^t(\omega_{m,\alpha}, \omega_{m-1,\beta}) = \bar{P}^t(\omega_{m,\beta}, \omega_{m-1,\alpha}) &= \frac{1}{L_\alpha + L_\beta}
\end{aligned} \tag{S15}$$

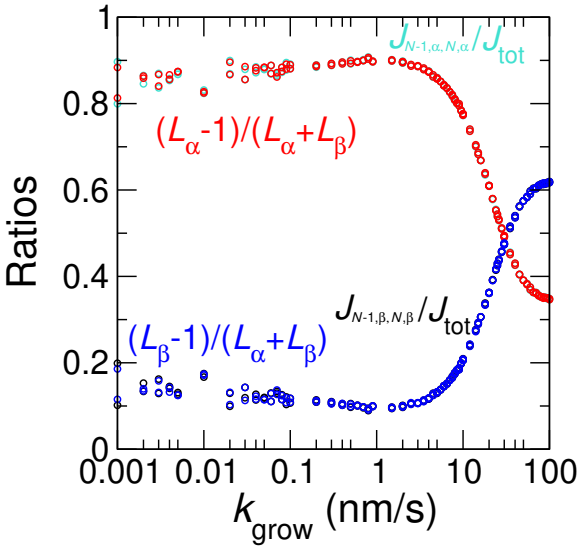

Figure S2. Comparison of currents and domain length ratios from KMC simulations at various actin polymerization rates. Both currents and domain lengths are measured from KMC simulations of 10^6 steps. The simulation parameters are the same as those used in generating Fig. 2.

Using Eq. (S14) and Eq. (S15), we obtain Eq. (6). Note that in main text we omit the ω's in the subscripts of the currents for clarity. The self-consistency conditions are validated by KMC simulations (Fig. S2).

D. Domain lengths predicted by master equation

Since the equilibrium parameters and the driving parts of the rates are determined, we now use the self-consistency condition above to solve the master equation (Eq. (5)) for the domain lengths L_α and L_β under non-equilibrium conditions.

$$\begin{aligned} L_\beta &= \frac{(L_\alpha-1)k^{f,2}_{\beta\alpha} - k^{f,2}_{\alpha\alpha}(L_\alpha(k^{f,2}_{\beta\alpha}+1)k^{f,1}_{\alpha\alpha}+L_\alpha-1)}{k^{f,2}_{\beta\alpha}k^{f,1}_{\alpha\alpha}(L_\alpha k^{f,2}_{\alpha\alpha}((1+k^{f,2}_{\alpha\beta})k^{f,1}_{\alpha\alpha}-(L_\alpha-1)k^{f,2}_{\alpha\beta}k^{f,1}_{\beta\beta})-(L_\alpha-1)(1+k^{f,2}_{\alpha\beta}+L_\alpha k^{f,2}_{\alpha\beta}k^{f,1}_{\beta\beta}))} \\ L_\alpha &= \frac{(L_\beta-1)k^{f,2}_{\alpha\beta} - k^{f,2}_{\beta\beta}(L_\beta(k^{f,2}_{\alpha\beta}+1)k^{f,1}_{\beta\beta}+L_\beta-1)}{k^{f,2}_{\alpha\beta}k^{f,1}_{\beta\beta}(L_\beta k^{f,2}_{\beta\beta}((1+k^{f,2}_{\beta\alpha})k^{f,1}_{\beta\beta}-(L_\beta-1)k^{f,2}_{\beta\alpha}k^{f,1}_{\alpha\alpha})-(L_\beta-1)(1+k^{f,2}_{\beta\alpha}+L_\beta k^{f,2}_{\beta\alpha}k^{f,1}_{\alpha\alpha}))} \end{aligned} \tag{S16}$$

We compute the domain lengths from Eq. (S16) numerically and compare them with those measured from KMC simulations in Fig. 2. We solve Eq. (S16) using standard numerical routines in MATHEMATICA [2].

For very low values of $k_{\rm grow} \approx 10^{-4}$ nm/s, the system is close to equilibrium and consequently the fluxes are also very small and their values are very sensitive to numerical errors. Under these conditions, it becomes tough to verify the mean-field approximation numerically. However, as we note in Fig. 2 (inset) the values of average domain lengths seem to be converging to their expected equilibrium values as $k_{\rm grow}$ is reduced. Hence, we expect the mean-field approximation to be valid close to equilibrium as well.

E. Dependence of the crossover in domain lengths on the binding affinities of ABPs

We have demonstrated that the master equation accurately predicts the domain lengths. Now we use it to investigate the dependence of the crossover in domain lengths on the equilibrium binding affinities of ABPs. We focus on the case in which binding of the α crosslinker is favored at equilibrium (i.e., $L_{\alpha,eq} > L_{\beta,eq}$) and tune the equilibrium binding affinities $k^{f,1}_{ij,eq}$ of ABPs to delineate the range over which the crossover occurs (Fig. S3). Beyond this range, either L_α is still larger than L_β in fast growing bundles, or L_α is already smaller than L_β very close to equilibrium. We find that the crossover of domain lengths is deferred to a faster growth speed when the binding affinity of the β crosslinker, $k^{f,1}_{\beta\beta,eq}$, is weakened, in agreement with previous simulation results in Ref. [3].

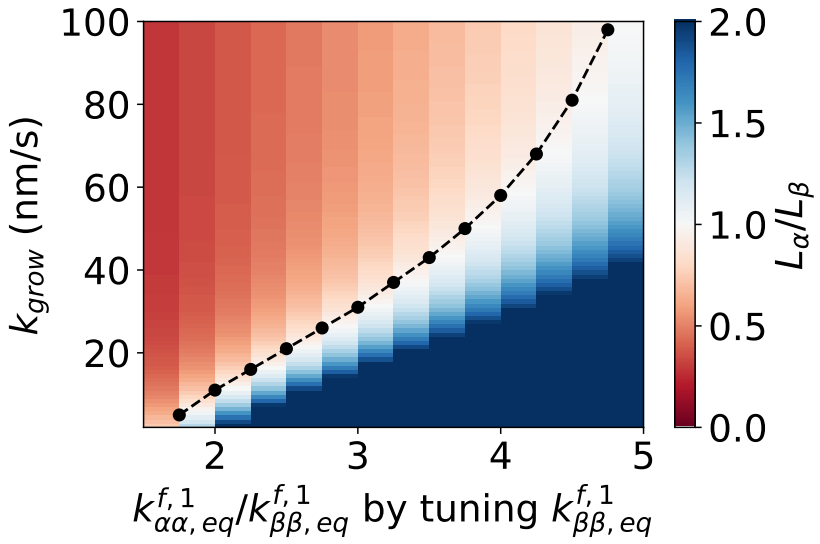

Figure S3. The dependence of domain length ratio L_α/L_β on the equilibrium binding rates $k^{f,1}_{\alpha\alpha,eq}/k^{f,1}_{\beta\beta,eq}$. Blue and red regions represent $L_\alpha > L_\beta$ and $L_\alpha < L_\beta$, respectively. Black dots and dashed lines mark the crossover of domain lengths, where $L_\alpha = L_\beta$. Simulation parameters are the same as those used in generating Fig. 2 except $k^{f,1}_{\beta\beta,eq}$, which is varied. Domain length ratios are computed from the master equation.

S2. DERIVATION OF EQ. (8-9)

The entropy production along the edge that links states i and j with forward rate k_{ij} and backward rates k_{ji} can be written as $J_{ij}\log\frac{k_{ij}P_i}{k_{ji}P_j}$, where J_{ij} is the flux along this edge. This allows us to express the entropy production rate of this process as

$$\dot{\sigma} = J_{N-1,\alpha,N,\alpha}\log\frac{k^{f,1}_{\alpha\alpha}k^{f,2}_{\alpha\alpha}}{k^{b,1}_{\alpha\alpha}k^{b,2}_{\alpha\alpha}} + J_{N-1,\beta,N,\beta}\log\frac{k^{f,1}_{\beta\beta}k^{f,2}_{\beta\beta}}{k^{b,1}_{\beta\beta}k^{b,2}_{\beta\beta}} + J_{N-1,\alpha,N,\beta}\log\frac{k^{f,1}_{\alpha\beta}k^{f,2}_{\alpha\beta}k^{f,1}_{\beta\alpha}k^{f,2}_{\beta\alpha}}{k^{b,1}_{\beta\beta}k^{b,2}_{\beta\beta}k^{b,1}_{\beta\alpha}k^{b,2}_{\beta\alpha}}. \tag{S17}$$

We then use the relation between domain lengths and currents in Eq. (6) to re-write Eq. (S17) as:

$$\dot{\sigma} = J_{\rm tot}\left(\frac{L_\alpha-1}{L_\alpha+L_\beta}\log\frac{k^{f,1}_{\alpha\alpha}k^{f,2}_{\alpha\alpha}}{k^{b,1}_{\alpha\alpha}k^{b,2}_{\alpha\alpha}} + \frac{L_\beta-1}{L_\alpha+L_\beta}\log\frac{k^{f,1}_{\beta\beta}k^{f,2}_{\beta\beta}}{k^{b,1}_{\beta\beta}k^{b,2}_{\beta\beta}} + \frac{1}{L_\alpha+L_\beta}\log\frac{k^{f,1}_{\alpha\beta}k^{f,2}_{\alpha\beta}k^{f,1}_{\beta\alpha}k^{f,2}_{\beta\alpha}}{k^{b,1}_{\beta\beta}k^{b,2}_{\beta\beta}k^{b,1}_{\beta\alpha}k^{b,2}_{\beta\alpha}}\right). \tag{S18}$$

To further simplify the expression above, we insert Eq. (S1) and obtain the following expression for entropy production rate,

$$\dot{\sigma} = J_{\rm tot}\left(\frac{2}{L_{\rm tot}}\sum_{i\in\alpha,\beta}L_i\log dk_i + \frac{1}{L_{\rm tot}}\sum_{i\in\alpha,\beta}L_i\log\frac{L_i}{L_{i,\rm eq}} - \frac{1}{L_{\rm tot}}\sum_{i\in\alpha,\beta}(L_i-1)\log\frac{L_i-1}{L_{i,\rm eq}-1}\right). \tag{S19}$$

The first term in the parenthesis in Eq. (S19) contains the driving parts, which we call $\Delta\mu$ as in Eq. (8). The two other terms represent the energy used in changing the morphology, which we refer to as ε_{diss} as in Eq. (9). Thus, the entropy production rate can be written in the following format, consistent with the expression used in Ref. [4] and also in Eq. (7).

$$\dot{\sigma} = J_{\rm tot}(\Delta\mu - \varepsilon_{diss}). \tag{S20}$$

S3. DERIVATION OF EQ. (1)

In this section, we derive Eq. (1) of the main text. Our derivation closely follows those in Refs. [5, 6]. As in the main text, we focus of experimentally accessible currents J_α and J_β related to the net rate at which the different crosslinkers are assimilated into the bundle. In particular, using the notation in Fig. S4, we have

$$\begin{aligned} J_\alpha &= [j(1) + j(4) + j(5) + j(8)]/2 \\ J_\beta &= [j(2) + j(3) + j(6) + j(7)]/2, \end{aligned} \tag{S21}$$

where we use $j(\epsilon)$ to denote the current along the edge ϵ.

Eq. (S21) can be written in matrix form as

$$J(n) = \sum_\epsilon j(\epsilon) d(\epsilon, n) \tag{S22}$$

where $d(n, \epsilon)$ are elements in a matrix $\mathbf{d}$ that describes how each of the generalized currents depends on the edge currents. For the specific case described above in Eq. (S21), the $\mathbf{d}$ matrix can be written as:

$$\mathbf{d}^T = \frac{1}{2} \begin{pmatrix} 1 & 0 & 0 & 1 & 1 & 0 & 0 & 1 \\ 0 & 1 & 1 & 0 & 0 & 1 & 1 & 0 \end{pmatrix} \tag{S23}$$

Before proceeding further, we outline the structure of the proof. We attempt to derive Eq. (1) by deriving constraints on the fluctuations of J_α and J_β (or equivalently $J(n)$ in Eq. (S22)). To do so we first express $J(n)$ in terms of the edge currents $\tilde{j}(\epsilon)$ such that $\tilde{j}(\epsilon)$ are guaranteed to satisfy current conservation, and they satisfy $J(n) = \sum_\epsilon \tilde{j}(\epsilon) d(\epsilon, n)$. Then, we use the findings of Ref. [5] which showed that the large deviation rate functions associated with the fluctuations in the various edge currents satisfy the following inequality,

$$I(\mathbf{j}) \leq \sum_\epsilon \left(j(\epsilon) - j^\pi(\epsilon)\right)^2 \frac{\sigma^\pi(\epsilon)}{4[j^\pi(\epsilon)]^2}, \tag{S24}$$

where $I(\mathbf{j})$ is the rate function of the edge currents, j^π is the average current of the edge and $\sigma^\pi(\epsilon)$ is the entropy production of edge ϵ. Note that the entropy production along the edge ϵ that links states i and j with forward rate k_{ij} and backward rates k_{ji} can be written as $\sigma^\pi(\epsilon) = j^\pi(\epsilon) \log \frac{k_{ij} P_i}{k_{ji} P_j}$. The sum of entropy production along all the edges should result in the total entropy as in Eq. (S18). Finally, by writing Eq. (S24) in terms of the generalized currents $J(n)$, we obtain our central result.

We now proceed by first "inverting" Eq. (S22) and defining a set of edge currents:

$$\tilde{j}(\epsilon) = \sum_n J(n) G(n, \epsilon) \tag{S25}$$

where $\mathbf{G}$ is a pseudoinverse of the matrix $\mathbf{d}$. Note that since $\mathbf{G}$ and $\mathbf{d}$ are pseudoinverses of one another, we have

$$\sum_\epsilon \tilde{j}(\epsilon) d(\epsilon, k) = \sum_{n,\epsilon} J(n) G(n, \epsilon) d(\epsilon, k) = \sum_{n,\epsilon,\epsilon'} j(\epsilon') d(\epsilon', n) G(n, \epsilon) d(\epsilon, k) = \sum_{\epsilon'} j(\epsilon') d(\epsilon', k) = J(k) \tag{S26}$$

Eq. (S26) suggests that the sets of currents $\tilde{\mathbf{j}}$ do not have to be identical to $\mathbf{j}$. We construct a specific matrix $\mathbf{G}$ below in Eq. (S34) which ensures that the resulting sets of currents $\tilde{\mathbf{j}}$ meet the following two requirements: first, the sets of $\tilde{\mathbf{j}}$ satisfy current conservation; second, the resulting sets of $\tilde{\mathbf{j}}$ at steady state match $\mathbf{j}$ at steady state. We can then use the arguments in Ref. [5, 6] to substitute Eq. (S25) into Eq. (S24) and obtain a bound on the large deviation rate function associated with the generalized currents, $I(\mathbf{J})$

$$I(\mathbf{J}) \leq \sum_\epsilon \left(\sum_n J(n) G(n, \epsilon) - J^\pi(\epsilon) G(n, \epsilon) \right)^2 \frac{\sigma^\pi(\epsilon)}{4[j^\pi(\epsilon)]^2}. \tag{S27}$$

Now we consider the system at steady state, with $\mathbf{J}^\pi$ denoting the vector of average generalized currents and $\mathbf{L}$ denoting the covariance of generalized currents. The rate function $I(\mathbf{J})$ can be expanded around the average generalized

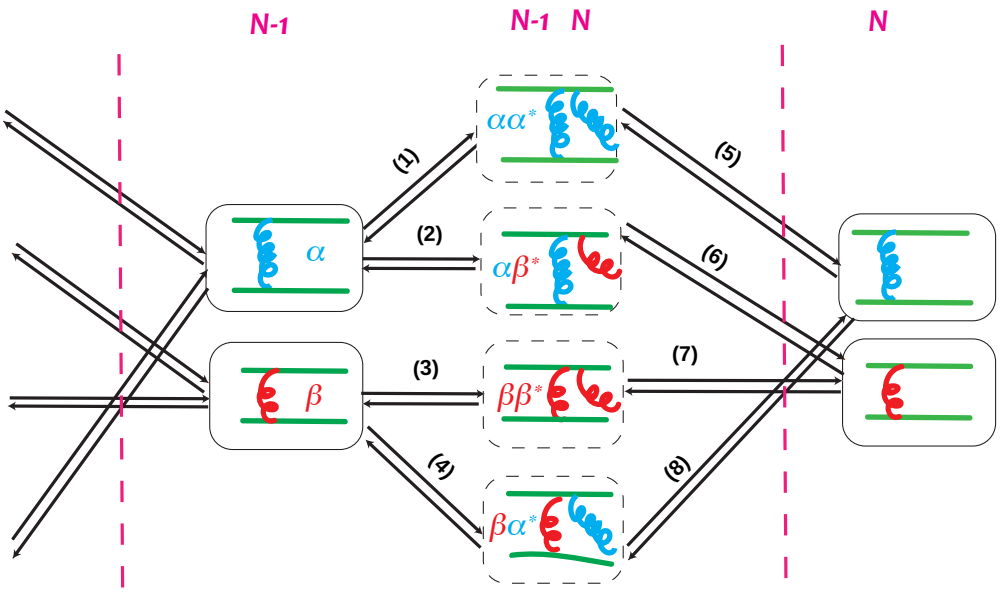

Figure S4. Schematic showing all the possible transitions of the actin bundle system. We index the graph edges from 1 to 8.

currents, $\mathbf{J}^\pi$, as

$$I(\mathbf{J}) \approx I(\mathbf{J}^\pi) + D\left[I(\mathbf{J})|\mathbf{J}^\pi\right] \cdot \tilde{\mathbf{J}} + \frac{1}{2}\tilde{\mathbf{J}}^T \cdot H\left[I(\mathbf{J})|\mathbf{J}^\pi\right] \cdot \tilde{\mathbf{J}} \tag{S28}$$

Here $\tilde{\mathbf{J}}$ is a vector with elements $(J(n) - \mathbf{J}^\pi(n))$, and $D\left[I(\mathbf{J})|\mathbf{J}^\pi\right]$ is the vector containing the derivatives of the rate function $I(\mathbf{J})$ with respect to the current $\mathbf{J}$. Since the rate function is at its minimum at $\mathbf{J}^\pi$, $I(\mathbf{J}^\pi)$ and $D\left[I(\mathbf{J})|\mathbf{J}^\pi\right]$ equal zero. $H\left[I(\mathbf{J})|\mathbf{J}^\pi\right]$ is the Hessian matrix of $I(\mathbf{J})$ evaluated at $\mathbf{J}^\pi$ which can be related to the covariance matrix $\mathbf{L}$ by [7]

$$H\left[I(\mathbf{J})|\mathbf{J}^\pi\right] = \mathbf{L^{-1}}. \tag{S29}$$

Eq. (S28) and Eq. (S29) then allow us to rewrite Eq. (S27) as

$$\tilde{\mathbf{J}}^T \cdot \mathbf{L}^{-1} \cdot \tilde{\mathbf{J}} \leq \tilde{\mathbf{J}}^T \cdot \mathbf{GSG^T} \cdot \tilde{\mathbf{J}} \tag{S30}$$

Here $\mathbf{G}$ is the matrix form of $G(n, \epsilon)$ with n indicating the row and ϵ indicating the column, $\mathbf{G^T}$ is its transpose and $\mathbf{S}$ is a diagonal matrix with elements $\sigma^\pi(\epsilon)/2|j^\pi(\epsilon)|^2$. Since Eq. (S27) is valid for any arbitrary fluctuation about the mean, $\mathbf{GSG}^T - \mathbf{L}^{-1}$ has to be positive semi-definite, which is to say that all of its eigenvalues have to be non-negative. For a 2×2 matrix, this is equivalent to

$$\mathrm{Tr}(\mathbf{GSG}^\mathrm{T} - \mathbf{L}^{-1}) \geq 0, \quad \mathrm{Det}(\mathbf{GSG}^\mathrm{T} - \mathbf{L}^{-1}) \geq 0. \tag{S31}$$

To finish the proof, we need to fix the matrix $\mathbf{G}$. The choice of $\mathbf{G}$ is guided by the fact that the inequality in Eq. (S27) is only valid when the currents $\tilde{\mathbf{j}}$ are conserved currents, which means the sum of the currents that go through each node is zero. This gives the following constraints on the edge currents $\tilde{j}_i$ (with the notation as specified in Fig. S4).

$$\tilde{j}(1) = \tilde{j}(5), \quad \tilde{j}(3) = \tilde{j}(7), \quad \tilde{j}(2) = \tilde{j}(4) = \tilde{j}(6) = \tilde{j}(8). \tag{S32}$$

These constraints require that the elements in $\mathbf{G}$ have the following relations.

$$G(i,1) = G(i,5), \quad G(i,3) = G(i,7), \quad G(i,2) = G(i,4) = G(i,6) = G(i,8) \tag{S33}$$

where $i = 1$ or 2 are the first and second row of $\mathbf{G}$ and represent the contributions of α and β components of the generalized currents to the edge currents.

The following $\mathbf{G}$ matrix written in terms of L_α and L_β satisfies all the constraints and is also a psuedoinverse of the $\mathbf{d}$ matrix:

$$\mathbf{G} = \frac{1}{(L_\alpha + L_\beta)} \begin{pmatrix} L_\alpha + L_\beta - 1 & 1 & -1 & 1 & L_\alpha + L_\beta - 1 & 1 & -1 & 1 \\ -1 & 1 & L_\alpha + L_\beta - 1 & 1 & -1 & 1 & L_\alpha + L_\beta - 1 & 1 \end{pmatrix}. \tag{S34}$$

Substituting the above equation into $\mathbf{GSG}^T$ and collecting the terms with $\ln dk_{\alpha/\beta}$ gives us the matrix $\boldsymbol{\delta\mu}$ in the main text. The rest is the matrix $\mathbf{D}$ in main text.

S4. DERIVATION OF THE LINEAR RESPONSE LIKE IDENTITY

A fluctuation dissipation like form can also be obtained as in Eq. (13) of the main text. In this section, we derive Eq. (13) using the matrix $\mathbf{GSG}^T$ we determined in Section S3. First, we multiply the matrix $\mathbf{GSG}^T$ by the vector $\mathbf{J}$ on both sides:

$$\mathbf{J}^T\mathbf{GSG}^T\mathbf{J} = \mathbf{j}^T\mathbf{Sj} = \dot{\sigma}/2 \tag{S35}$$

with $\mathbf{J}^T = (J_\alpha, J_\beta)$ and $\mathbf{j}^T = (j_1, j_2, ..., j_8)$. The entropy production can be further rewritten as:

$$\dot{\sigma} = J_{\text{tot}}(\Delta\mu - \varepsilon_{diss}) = 2\mathbf{J}^T\left(\mathbf{dk} - \mathbf{D}[\mathbf{p}]\right) \tag{S36}$$

where the microscopic force vector $\mathbf{dk}$ and the relative entropy term $\mathbf{D}[\mathbf{p}]$ are defined as

$$\begin{aligned} \mathbf{dk} &= \begin{pmatrix} \log dk_\alpha \\ \log dk_\beta \end{pmatrix} \\ \mathbf{D}[\mathbf{p}] &= \begin{pmatrix} D(P(\alpha)||P^{eq}(\alpha)) \\ D(P(\beta)||P^{eq}(\beta)) \end{pmatrix} \end{aligned} \tag{S37}$$

with

$$D(P(i)||P^{eq}(i)) = \frac{L_i - 1}{2L_i}(\log\frac{L_i - 1}{L_i} - \log\frac{L_{i,\text{eq}} - 1}{L_{i,\text{eq}}}) + \frac{1}{2L_i}(\log\frac{1}{L_i} - \log\frac{1}{L_{i,\text{eq}}}) \tag{S38}$$

We then arrive at:

$$\mathbf{J}^T\mathbf{GSG}^T\mathbf{J} = \mathbf{J}^T\left(\boldsymbol{\delta\mu} - \mathbf{D}\right)\mathbf{J} = \mathbf{J}^T\left(\mathbf{dk} - \mathbf{D}[\mathbf{p}]\right) \tag{S39}$$

So when $\boldsymbol{\delta\mu} - \mathbf{D} = \mathbf{L}^{-1}$, we obtain Eq. (13) in the main text.

S5. THE THERMODYNAMIC BOUND FOR DRIVING IS IMPROVED BY CONSIDERING INDIVIDUAL CURRENTS INSTEAD OF THE TOTAL CURRENT IN THE TUR

We plot the second law bound and the TUR bound (Eq. (16)) in Fig. 5. The TUR bound is much better than the second law bound because it encodes the kinetic information of the process. It deviates from simulation results at intermediate polymerization rate $k_{\text{grow}} = 1$ nm/s. For further improvement, we adapt the MTUR bound [8] to this process. We define the fluxes of adding α and β ABPs as $J_\alpha = J_{\omega_{m-1,\alpha},\omega_{m,\alpha}} + J_{\omega_{m-1,\beta},\omega_{m,\alpha}}$ and $J_\beta = J_{\omega_{m-1,\alpha},\omega_{m,\beta}} + J_{\omega_{m-1,\beta},\omega_{m,\beta}}$.The MTUR bound given by Eq. (15) is the same as considering the scalar observable $J_{tot'} = \cos\phi J_\alpha + \sin\phi J_\beta$ and then maximizing $\frac{2\langle J_{tot'}\rangle^2}{tJ_{\text{tot}}\langle\delta J^2_{tot'}\rangle}$ by varying ϕ. We demonstrate below the derivation and plot the $\tan\phi$ values that optimize the bound as a function of k_{grow}.

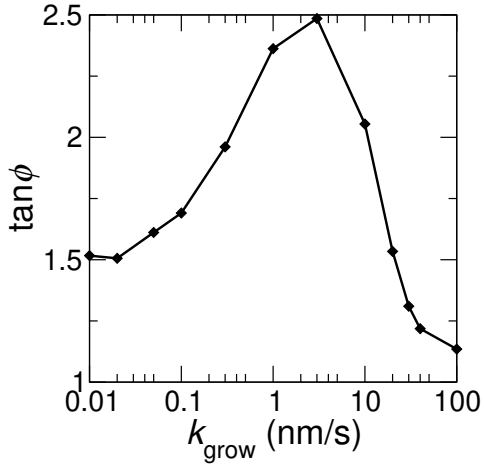

Figure S5. Coefficient $\tan\phi$ at various actin polymerization rates $k_{\rm grow}$. The parameters are the same as in Fig. 5.

Inserting the expression of $J_{tot'}$ into the bound of $\frac{2\langle J_{tot'}\rangle^2}{tJ_{\rm tot}\langle \delta J_{tot'}^2\rangle}$, we obtain

$$\Delta\mu \geqslant \varepsilon_{diss} + \frac{2(J_\alpha + \tan\phi J_\beta)^2}{tJ_{\rm tot}(\langle \delta {J_\alpha}^2\rangle + \tan^2\phi\langle \delta {J_\beta}^2\rangle + 2\tan\phi\langle \delta J_\alpha \delta J_\beta\rangle)} \tag{S40}$$

We take the derivative of Eq. (S40) against $\tan\phi$ and find that the maximum value is achieved when

$$\tan\phi = \frac{-\langle \delta J_\alpha \delta J_\beta\rangle J_\alpha + \langle \delta {J_\alpha}^2\rangle J_\beta}{-\langle \delta J_\alpha \delta J_\beta\rangle J_\beta + \langle \delta {J_\beta}^2\rangle J_\alpha}. \tag{S41}$$

We substitute Eq. (S41) for $\tan\phi$ in Eq. (S40) and obtain the following MTUR bound for the bundling process.

$$\Delta\mu \geqslant \varepsilon_{diss} + \frac{2(J_\alpha^2\langle \delta {J_\beta}^2\rangle - 2\langle \delta J_\alpha \delta J_\beta\rangle J_\alpha J_\beta + J_\beta^2\langle \delta {J_\alpha}^2\rangle)}{tJ_{\rm tot}(-\langle \delta J_\alpha \delta J_\beta\rangle^2 + \langle \delta {J_\alpha}^2\rangle\langle \delta {J_\beta}^2\rangle)}. \tag{S42}$$

This is equivalent to Eq. (15), where we simplify the expression using

$$\mathbf{J} = \begin{pmatrix} J_\alpha \\ J_\beta \end{pmatrix}, \mathbf{dk} = \begin{pmatrix} \log dk_\alpha \\ \log dk_\beta \end{pmatrix} \text{ and } \mathbf{D}[\mathbf{p}] = \begin{pmatrix} D(P(\alpha)||P^{eq}(\alpha)) \\ D(P(\beta)||P^{eq}(\beta)) \end{pmatrix}. \tag{S43}$$

Fig. S5 shows the value of $\tan\phi$ in Eq. (S41) at various $k_{\rm grow}$. This coefficient is obtained by maximizing the bound in Eq. (S40) at each data point. It provides information about the strength of the correlation between the two currents. We compare this bound with the one given by the TUR (Eq. (16)) in Fig. 5 and discuss their performance in the main text.

To further analyze how the variance and covariance of fluxes modulate the value of $\tan\phi$ and the amount of driving used to maintain the correlation between fluxes, we rearrange the expression of $\tan\phi$ as follows.

$$\tan\phi = \frac{J_\alpha}{J_\beta}\left[\frac{-\langle \delta J_\alpha \delta J_\beta\rangle}{J_\alpha J_\beta} + \frac{\langle \delta {J_\alpha}^2\rangle}{{J_\alpha}^2}\right]\left[\frac{-\langle \delta J_\alpha \delta J_\beta\rangle}{J_\alpha J_\beta} + \frac{\langle \delta {J_\beta}^2\rangle}{{J_\beta}^2}\right]^{-1} \tag{S44}$$

Fig. S5 shows that the ratio between currents J_α/J_β has the same non-monotonic dependence on actin polymerization rate as $\tan\phi$. This is consistent with Eq. (S44). On the other hand, the normalized variance and covariance of currents $-\langle \delta J_\alpha \delta J_\beta\rangle/J_\alpha J_\beta$, $\langle \delta {J_\alpha}^2\rangle/J_\alpha^2$ and $\langle \delta {J_\beta}^2\rangle/J_\beta^2$ have similar orders of magnitude for a given $k_{\rm grow}$ (Fig. S7), suggesting that the value of $\tan\phi$ is weakly dependent on the second and the third terms on the right side of Eq. (S44). We conclude that $\tan\phi$, as well as the strength of the correlation between fluxes is mainly determined by the ratio between the two currents.

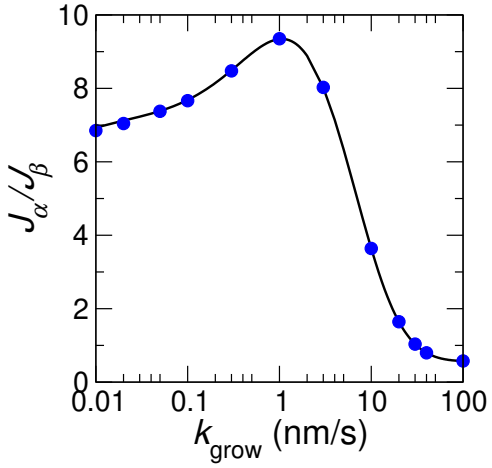

Figure S6. The ratio between the two currents J_α/J_β computed from KMC simulations (blue points) and predicted by the master equation (black curve).

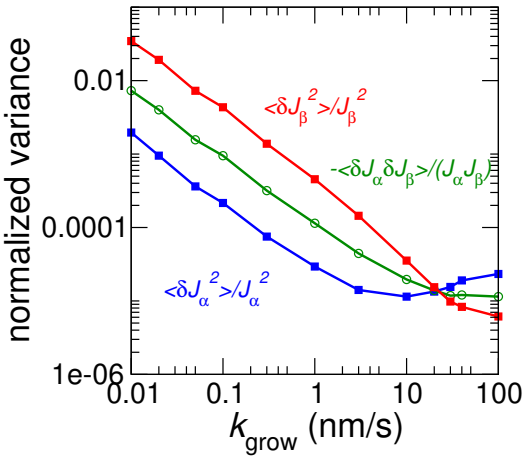

Figure S7. Normalized variance and covariance computed from KMC simulations. Blue and red points are the variance normalized by the corresponding current ($\langle \delta J_\beta^2 \rangle / J_\beta^2$ and $\langle \delta J_\alpha^2 \rangle / J_\alpha^2$) computed from simulations. Green points are the covariance normalized by the magnitude of the two currents ($-\langle \delta J_\alpha \delta J_\beta \rangle / J_\alpha J_\beta$).

[1] P. Gaspard and D. Andrieux, J. Chem. Phys. **141**, 044908 (2014).
[2] W. R. Inc., "Mathematica, Version 12.2," Champaign, IL, 2020.
[3] S. L. Freedman, C. Suarez, J. D. Winkelman, D. R. Kovar, G. A. Voth, A. R. Dinner, and G. M. Hocky, Proc. Natl. Acad. Sci. **116**, 16192 (2019).
[4] M. Nguyen and S. Vaikuntanathan, Proc. Natl. Acad. Sci. **113**, 14231 (2016).
[5] T. R. Gingrich, J. M. Horowitz, N. Perunov, and J. L. England, Phys. Rev. Lett. **116**, 120601 (2016).
[6] J. Yan, arXiv:1905.00929 (2019).
[7] R. S. Ellis, *Entropy, large deviations, and statistical mechanics* (Springer-Verlag, 1985).
[8] A. Dechant, J. Phys. A Math. **52**, 035001 (2018).